Renewable and Sustainable Energy Reviews 31 (2014) 289–304

Contents lists available at ScienceDirect

Renewable and Sustainable Energy Reviews

journal homepage: www.elsevier.com/locate/rser

Heat and flow characteristics of air heater ducts provided with turbulators—A review

Tabish Alam [a,*], R.P. Saini [a], J.S. Saini [b]

[a] *Alternate Hydro Energy Centre, Indian Institute of Technology Roorkee, Roorkee, Uttarakhand 247667, India*
[b] *Mechanical & Industrial Engineering Department, Indian Institute of Technology Roorkee, Roorkee, Uttarakhand 247667, India*

ARTICLE INFO

Article history:
Received 18 February 2013
Received in revised form
18 November 2013
Accepted 22 November 2013
Available online 18 December 2013

Keywords:
Heat exchanger
Solar air heater
Vortex generator
Rib
Perforation
Turbulator
Delta winglet

ABSTRACT

The use of turbulators in different forms of ribs, baffles, delta winglets, obstacles, vortex generator, rings and perforated blocks/baffles is an effective way to improve the performance of heat exchangers and solar air heaters. Investigators studied the effect of these turbulators for heat transfer and friction characteristics in air ducts. An attempt has been made in this paper to carry out an extensive literature review of turbulators used to investigate heat transfer augmentation and flow structure in air ducts. Based on the review it is found that perforation in ribs/baffles/blocks and combination of combined rib and delta winglet leads to the better thermo-hydraulic performance. The correlations presented by various investigators, in terms of non-dimensional parameters for heat transfer and friction factor in solar air heaters and heat exchangers have also been presented.

Contents

1. Introduction

Uses of energy are increasing with the population growth of the world with limited resources of energy such as crude oil, natural gas, coal and nuclear energy, etc. Continuous use of these resources would lead to dissipation. Conventional energy degradation with the consumption of fossil fuels is an intimidation to life on this earth. In view of earth's depleting fossil fuel reserves, researchers are stimulated to develop renewable energy available on earth. Of many renewable energies, solar energy is an epochal alternative as an unlimited source of energy which can fulfil the need of our daily life. The most dexterous way to utilise solar energy is to transform it into thermal energy by using solar air heater. Solar air heater is simple and less sophisticated in nature due to its simple design and low cost. The thermal efficiency of solar air heater is considered to be very low because of high thermal resistance or low heat transfer capability between absorber plate and flowing air in the duct. Various enhancement techniques are employed to make the solar air heater efficient. Enhancement techniques essentially reduce the thermal resistance in a conventional solar air heater by promoting higher convective heat transfer coefficient with or without increase in surface area. Number of techniques have been investigated and are available for enhancing the heat transfer rate in solar air heaters. Many investigators used fins, artificial roughness, and corrugated absorber plate to reduce the thermal resistance. Turbulators in the form of delta winglet, vortex generator, obstacles and perforated baffles/ribs/blocks

* Corresponding author. Tel.: +91 9411007747; fax: +91 1332 273517.
E-mail address: tabish.iitr@gmail.com (T. Alam).

1364-0321/$ - see front matter
http://dx.doi.org/10.1016/j.rser.2013.11.050

have been used for enhancing the convective heat transfer coefficient by creating turbulence at heat transfer surface. In this paper, an attempt has been made to review the investigation carried out by various investigators for heat and flow characteristics in ducts provided with different types of turbulators viz. solid ribs, perforated baffles/block/ribs, rings, vortex generator, obstacles and delta winglets.

2. Concept of turbulators using in air heater ducts

Turbulators in dynamic flow field of air create turbulence in flow and improve the heat transfer exchange by convection. The presence of the turbulators in fluid flow results in enhancement of heat transfer from the absorber plate with high penalty of pressure loss. The turbulators can create one or more combinations of the following conditions favourable to heat transfer rate with minimal pressure penalty such as (i) breaking the sub-laminar boundary, (ii) increasing the turbulent intensity, (iii) increase in heat transfer area, and (iv) generating of vortex and/or secondary flows. The turbulators of larger height are responsible for high heat transfer but are also responsible for high pressure drop. Due to recirculation of flow, hot zone is developed behind these elements leading to deterioration of heat transfer from these zones. Thus attempts have been made by the researchers in order to solve this problem by providing perforations in the ribs/block/baffles. The perforations enhance the heat transfer from these zones and reduce the pressure drop across the channel. The perforations in elements allow a part of the flow to pass through these perforations and mix with the main flow to create a higher level of mixing and turbulence. Nikuradse [1] attempted to develop temperature distribution and velocity in roughened air ducts and various researchers conducted experimental investigations on turbulators. Dipprey and Sabersky [2] experimentally investigated three sand grain roughened tubes and one smooth tube. Measurements of heat transfer and friction coefficients were obtained with distilled water flowing through electrically heated tubes. Increment in heat transfer due to roughness was found as high as 270%. Similar study carried out by Gomelauri [3] in which, roughened annulus tubes were examined. Kolar [4] tested roughened tube which was formed by cutting 60° triangular threads inside the tube. Sheriff and Gumley [5] investigated regular geometry to study the effect of roughness on heat transfer and friction factor. Webb et al. [6] investigated heat transfer and friction factor in tubes having repeated ribs. The heat transfer and friction factor correlations were developed for turbulent flow [7]. Heat transfer correlation was based on application of a heat–momentum transfer analogy proposed by Dipprey and Sabersky [2]. Developed correlations were used to define the performance advantage of roughened tubes in heat exchanger design in comparison to similar smooth tubes [8]. Donne and Meyer [9] performed the experiments to measure the heat transfer and friction coefficients of roughness with single rods contained in smooth tubes. Bergles et al. [10] reported enhancement techniques in heat transfer coefficient for heat exchangers. Thereafter many experimental investigations on enhancement of heat transfer have been performed in the area of heat exchanger, gas turbine, the aerofoil cooling system, gas cooled nuclear reactors and solar air heater.

3. Types of turbulators used in air heater duct

There are various types of turbulators evaluated and examined by various investigators in order to enhance the heat transfer. Surface geometry modifications in the form of turbulators change flow pattern on the heated surface and enable mixing of faster fluid region with the slower fluid region. Wakes at downstream side of turbulators introduced longitudinal trailing vortices in the boundary layer which break-up the laminar sub-layer or viscous sub-layer and increase the turbulence near the surface. Investigators have used turbulators in the form of solid ribs/baffles/blocks, perforated ribs/perforated/blocks, delta winglets, obstacles and vortex generator, etc. The classifications of different types of turbulators are shown in Fig. 1.

3.1. Solid ribs/baffles/blocks

Turbulators in the form of transverse, angled, V-shaped and W shaped ribs were widely investigated. These ribs may be used as continuous, broken and combination of both. Geometric parameters such as channel aspect ratio (AR), rib aspect ratio, rib height to channel height ratio, rib height to pitch ratio, channel width to height ratio, rib height to passage hydraulic diameter (e/D_h), rib angle of attack (α), rib positions, rib shape and type of rib (solid, perforated and slit rib, etc.) have pronounced effects on both local and overall heat transfer coefficients. Local Nusselt number distribution over flat and ribbed surface in a flow channel had been reported by Das [11].

Han et al. [12] investigated the turbulators ribs in rectangular channels of narrow aspect ratios and found that narrow aspect ratio channels gave better heat transfer than the wide aspect ratio channels for a constant pumping power. Han et al. [13] further reported that ribs at an angle of attack of 45° were found to have better performance at a given frictional power when compared with transverse ribs. Firth and Meyer [14] compared the heat transfer and friction performance for four different roughened

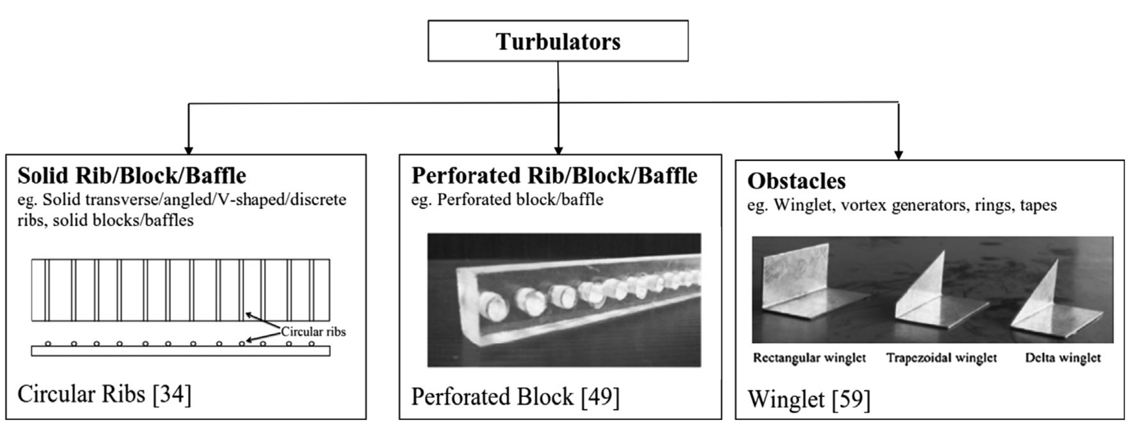


Fig. 1. Classification of turbulators used in air heater.

surfaces namely, square transverse ribbed surface, helically ribbed surface, trapezoidal transverse ribbed surface and three dimensional surface. The best overall performance was given by three dimensional surfaces. Han and Park [15,16] determined the effects of the angle of attack and channel aspect ratio on local heat transfer coefficient and friction factor with a pair of opposite rib-roughened walls for Reynolds number (Re) from 10,000 to 60,000. The highest heat transfer and pressure drop were found at angle of attack (α) of 60° with channel aspect ratio of 2.

Park et al. [17] tested the turbulence promoters in the form of angled ribs attached on opposite walls of rectangular channel. Investigation encompassed the effect of the channel aspect ratio (e/H), angle of attack (α), and flow Reynolds number (Re). It was observed that narrow aspect ratio (e/H) channels gave better heat transfer than the wide aspect ratio (e/H) channels. However, ribs with an angle of attack of 60°/45° provided the best heat transfer performance in wide aspect ratio channels. Hong and Hsieh [18] conducted the experiment in which the ribs were attached in a staggered manner to determine the heat characteristics. The values of relative rib height (e/D_h) and relative pitch ratio (p/e) were considered as 0.19 and 5.31 respectively. The heat transfer rate was found to be 2.02–4.60 times as that of smooth duct for lower Reynolds number.

Facchini et al. [19] investigated heat transfer and pressure drop in flows through ribbed channel for different values of aspect ratio of rib roughened channel for a rib angle of 60°. Khan et al. [20] also investigated square ribbed at a rib pitch ratio of 10. Mean temperature of ribbed duct has been found to be increased by 2.45% at Reynolds number of 50,000 over a smooth duct, whereas in the ribbed duct Nusselt number increased by 15.14% than that of the smooth duct with a 6% increase in pressure drop. Liu et al. [21] studied heat transfer characteristics of a rectangular channel having two opposite rib-roughened walls. Experiments conducted for different values of Reynolds number (Re), pitch to rib height, channel aspect ratio (W/H), rib angle of attack and channel blockage ratio in the range of 10,000–80,000, 0.25–1, $45° - 60°$ and 0.047–00.5 respectively. The geometries are shown in Fig. 2.

Liou and Hawang [22] explored the effect of various shaped ridges mounted on two opposite walls of channel on heat transfer and friction. Shapes of the ridge cross section were tested, namely triangular shape, semi-circular shape and square shape. They showed that square shaped ridges had highest heat transfer while semi-circular shaped ridges had minimum heat transfer.

Sparrow and Charmchi [23] carried out analytical study on heat transfer and laminar flow in duct having periodic corrugations distributed across the span while other bounding wall was smooth and parallel to corrugated wall. They concluded that corrugated duct was efficient when duct having lower wall temperature. Further, Sparrow and Hossfeld [24] investigated the effects of rounding of the peaks of corrugated-wall duct on heat transfer and pressure drop. It was reported that the rounding of the corrugation peaks resulting in decrease of both Nusselt number (Nu) and friction factor.

Sara et al. [25] carried out an experimental study to enhance the heat transfer from flat surface in a flow channel provided with rectangular cross sectional blocks. The blocks were positioning both transverse and parallel (inline and staggered) with respect to main flow direction as shown in Fig. 3. It was found that heat transfer depends on the spacing between the blocks, positioning and their arrangement. Parallel arrangement of blocks in staggered manner was found to be the optimised arrangement.

Won et al. [26] investigated the angled rib turbulators having an angle of attack 45°, rib height to hydraulic diameter ratio of 0.078, rib pitch to height ratio of 10 and a blockage of 25% for a Reynolds number range of 9000–76,000.

Tanda [27] investigated the effect of repeated (continuous and broken) ribs having rib pitch to height ratio of 8 and 13.3 V-shaped with 45° or 60° relative to flow direction (Fig. 4). Considerable heat transfer for a range of Reynolds number varying from 8900 to 36,000 has been found. It was found that the features of the inter-rib distribution on heat transfer coefficient are strongly related to rib shape and geometry.

Wang and Sunden [28] investigated heat transfer and fluid flow characteristics in a rectangular channel provided broken V-shaped ribs pointing upstream for a Reynolds number range of 1000–6000. Better heat transfer has been found with broken ribs as compared to continuous ribs. Wang and Sunden [29] further investigated the effect of continuous and truncated ribs attached on one wall of square duct for Reynolds number range from 8000 to 20,000. Continuous ribs gave a better heat transfer augmentation with increased pressure drop in comparison of truncated ribs. The effect of 90° continuous, 90° saw tooth profiled and 60° V-broken ribs on local heat transfer distribution was studied by Gupta et al. [30]. It was observed that 60° V-broken ribs had higher average heat transfer than that of 90° saw tooth profiled ribs and 90° continuous ribs. Maurer et al. [31] investigated the thermal

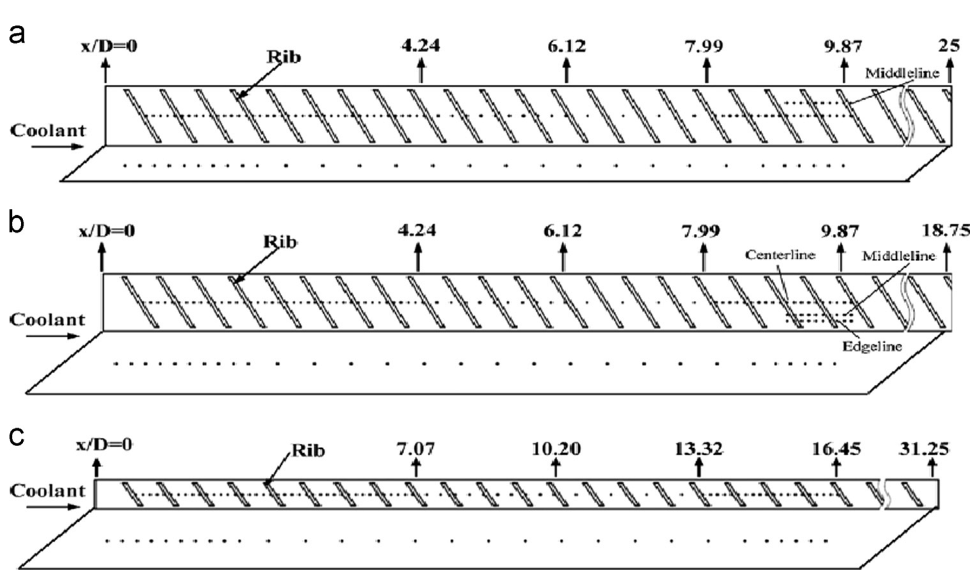


Fig. 2. Rib roughened wall: (a) $W/H=1.0$, (b) $W/H=0.5$, and (c) $W/H=0.25$ [22].

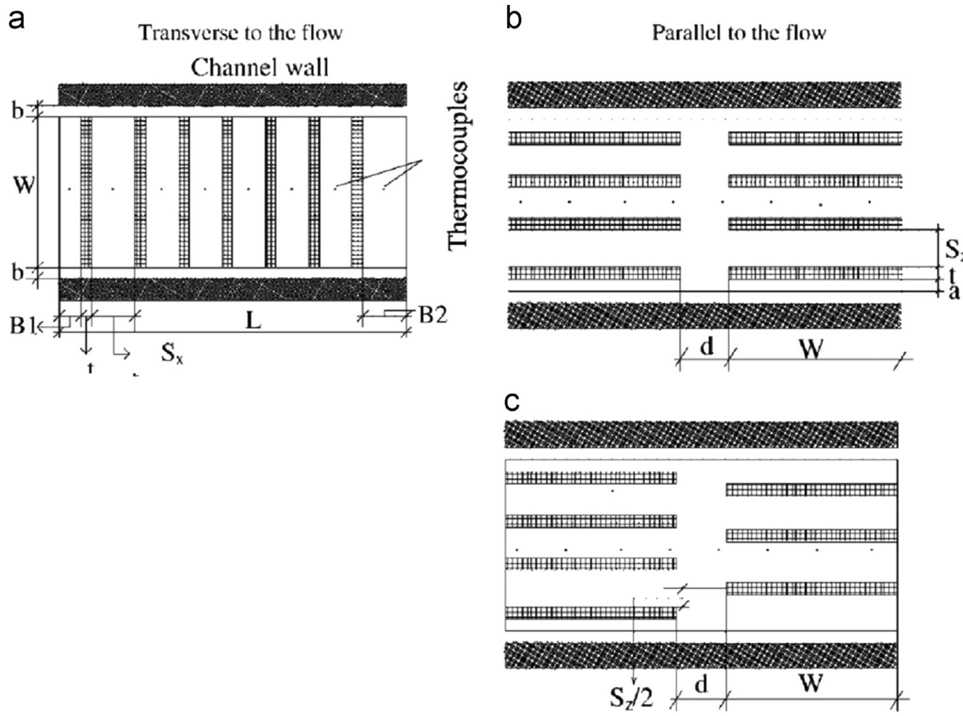


Fig. 3. Arrangement of block in flow channel [26]. (a) Block transverse to the flow, (b) blocks parallel to the flow-in line arrangement and (c) blocks parallel to the flow-staggered arrangement.

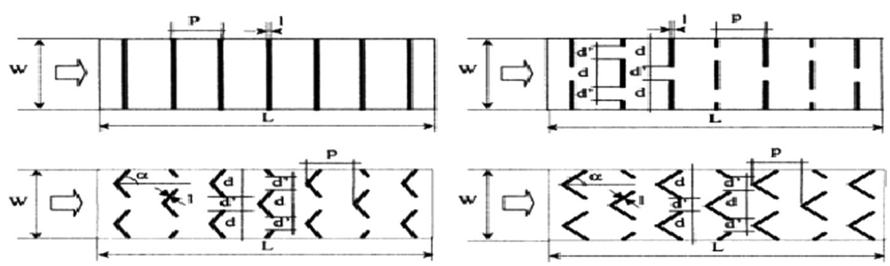


Fig. 4. Geometry of rib configurations: (1) transverse continuous ribs; (2) transverse broken ribs; (3) broken 60° V-ribs; and (4) broken 45° V-ribs [27].

performance of V-shaped and W-shaped ribs provided one side or on both sides of the test channel for a Reynolds number ranging from 80,000 to 500,000. W-shaped ribs have been found to have better heat transfer and with pressure drop. Lesley et al. [32] studied the heat transfer distribution and friction loss in a roughened channel with angled, V-shaped, W-shaped (full and discrete ribs). Overall thermal performance found to be better for discrete V-shaped and discrete W-shaped ribs in comparison to continuous V and W shaped ribs.

Lau et al. [33] examined the turbulent heat transfer and friction characteristics of fully developed flow in square channel having two opposite walls with attached ribs. The geometry of ribs namely, 90° full ribs, 60° full ribs, 45° V-shaped ribs, 60° V-shaped ribs, 135° V-shaped ribs and 60°/120° crossed ribs were tested as shown in Fig. 5. Highest heat transfer per unit pumping power was observed for 60° V-shaped ribs. Han and Zhang [34] explored the effect of broken rib orientation on local heat transfer distribution and pressure drop in square channel with two opposite in-line ribbed walls. Twelve configurations namely, 90° continuous rib, 90° broken rib, 60° parallel broken rib, 45° parallel broken rib, 60° V-shaped broken rib, 45° V-shaped broken rib, 60° V-shaped broken rib A, 45° V-shaped broken rib A, 60° parallel continuous rib, 45° parallel continuous rib, 60° V-shaped continuous rib and 45° V-shaped continuous rib were tested. It was found that 60° parallel broken ribs provided a higher heat transfer

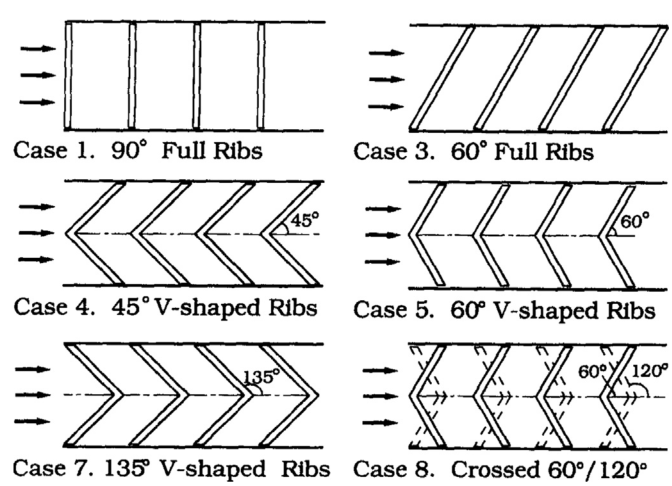


Fig. 5. Different ribs geometry configurations [33].

augmentation than 45° V-shaped broken rib and 60° V-shaped continuous rib. The rib configurations are shown in Fig. 6.

Smith and Promvonge [35] reported the combined effects of rib grooved turbulators on the heat transfer and friction

characteristics of a rectangular duct under a uniform heat flux condition. Three distinct configurations were tested namely rectangular rib with triangular grove, triangular rib with rectangular grove, and triangular rib with triangular grove in a duct for Reynolds number range varying from 3000 to 10,000. It was reported that rectangular rib with triangular grove arrangement provided maximum heat transfer rate and friction factor.

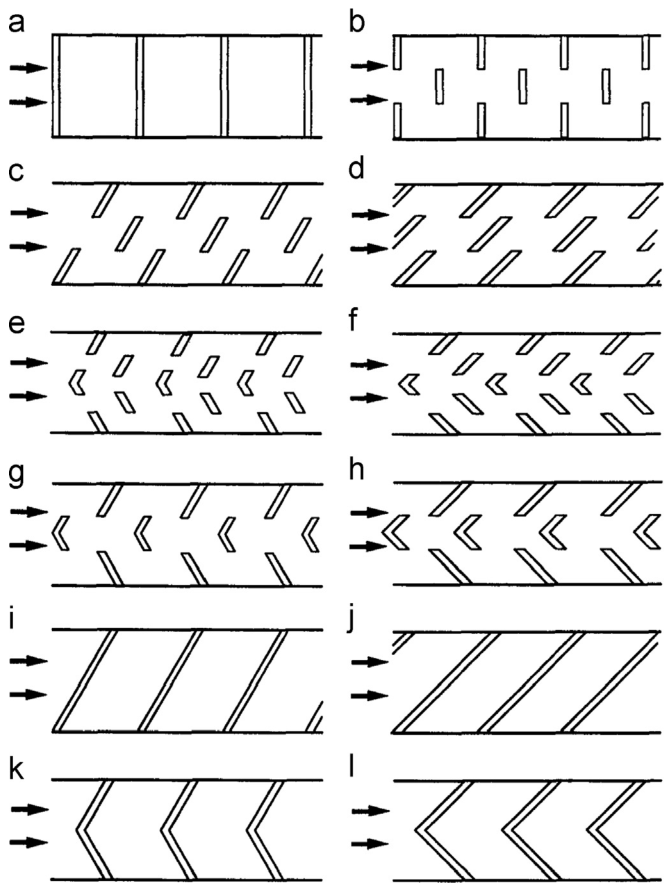


Fig. 6. Continuous and broken rib configurations [34]. (a) 90° continuous rib, (b) 90° broken rib, (c) 60° parallel broken rib, (d) 45° parallel broken rib, (e) 60° V - shaped broken rib, (f) 45° - shaped broken rib, (g) 60° V - shaped broken rib - A, (h) 45° V - shaped broken rib - A, (i) *60° parallel continuous rib, (j) *45° parallel continuous rib, (k) *60° V - shaped continuous rib and (l) *45° V - shaped continuous rib.

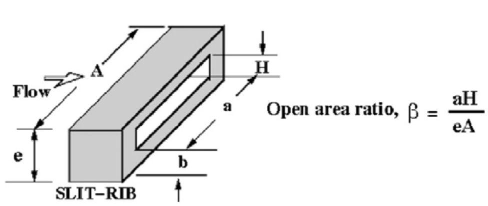


Fig. 7. Square rib with a slit [36].

Tariq et al. [36] investigated the effect of rib with a continuous slit as shown in Fig. 7 on heat transfer for Reynolds number ranging from 22,600 to 40,800. Nusselt number has been found to have strong dependence on the open area ratio and recirculation. The results were shown as Panigrahi et al. [37] investigated the effect of permeable rib geometries (solid, slit, split-slit and inclined split-slit ribs) for a Reynolds number of 5538. Reattachment length has been found to be a strong parameter for the heat transfer.

Chaube et al. [38] studied the nine distinct geometries (square, rectangular, chamfered, semi-circular and circular rib, etc.) for a Reynolds number ranging from 3000 to 20,000 in a solar air heater. A better heat transfer was achieved with chamfered ribs, however the best performance index is found to be with rectangular rib. Promvonge and Thianpong [39] also investigated the different shaped ribs (triangular or isosceles, wedge shaped or right angle triangular and rectangular) on heat transfer and friction loss behaviour in a rectangular channel for Reynolds number ranging from 4000 to 16,000 as shown in Fig. 8. Triangular shaped ribs have been found to have better performance than rectangular ones. Kamali and Binesh [40] studied turbulent heat transfer and friction in a square duct having three different shaped ribs (square, triangular and trapezoidal) as shown is Fig. 9. It was observed that heat transfer coefficient was strongly dependent on shape of ribs and heat transfer enhancement was found to be maximum for trapezoidal ribs.

Yeh and Chou [41] improved the collector efficiency of solar air heater duct by attaching the fins with baffles on the underside of collector. It was observed that there was considerable improvement in collector efficiency but at high pressure drop of air across the collector. This enhancement in collector efficiency further increased with increasing the density of baffles. Promvonge [42] carried out investigation in a duct having multiple 60° V-baffles tabulator as shown in Fig. 10. Baffle having blockage ratios (e/H) range from 0.1 to 0.3 and pitch ration (p/H) from 1 to 3 were tested. It was found that V-baffle provided considerable increment in Nusselt number, friction factor and thermal enhancement factor values over the smooth wall channel. Sriromreun et al. [43] investigated the effect of zigzag shape baffles (Z-shaped baffle) aligned in series (Fig. 11). It was observed that Nusselt number,

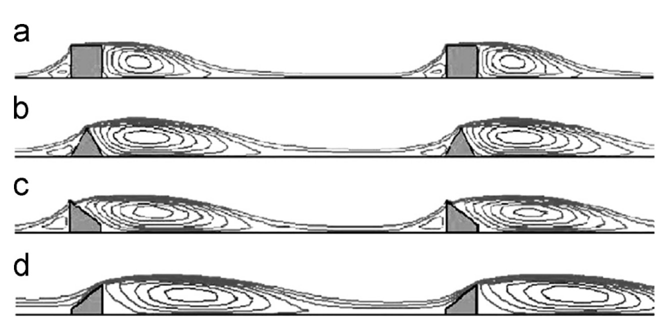


Fig. 9. Flow over ribs [40].

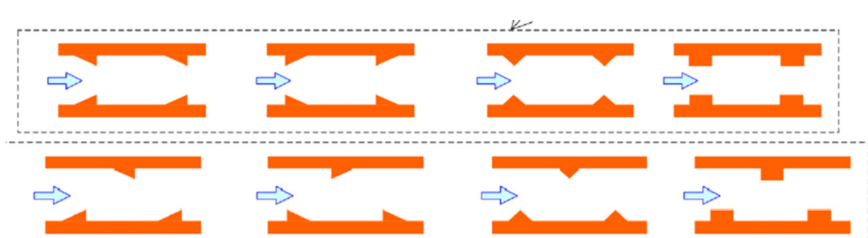


Fig. 8. Different staggered ribs array [39].

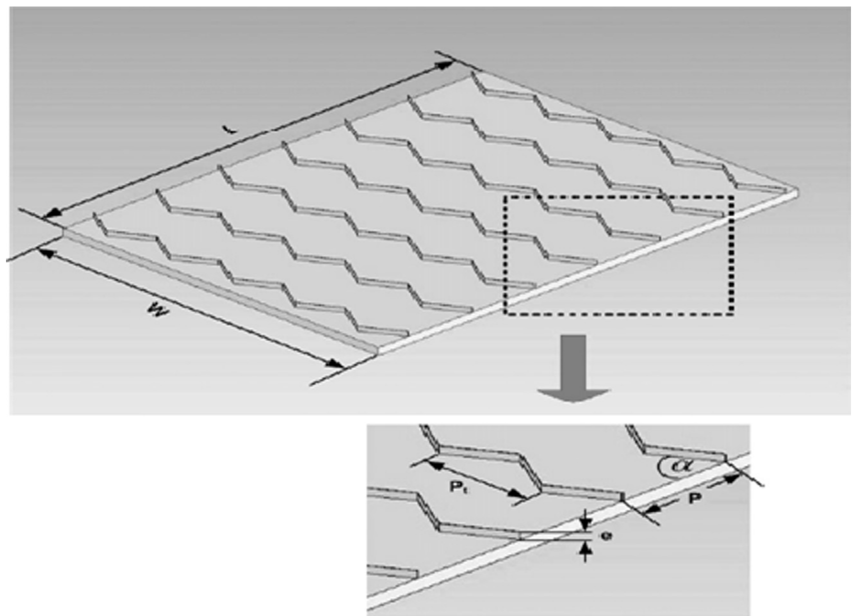


Fig. 10. Multiple 60° V-baffles [42].

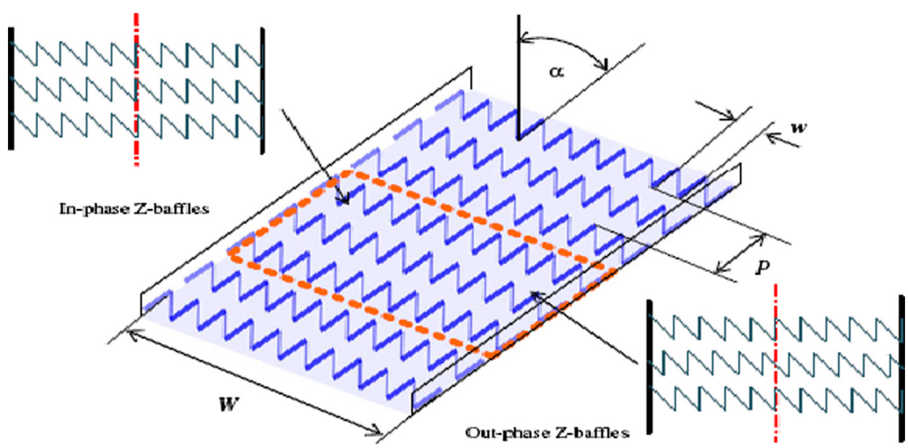


Fig. 11. Test section with in-phase and out-phase Z-baffle arrangements [43].

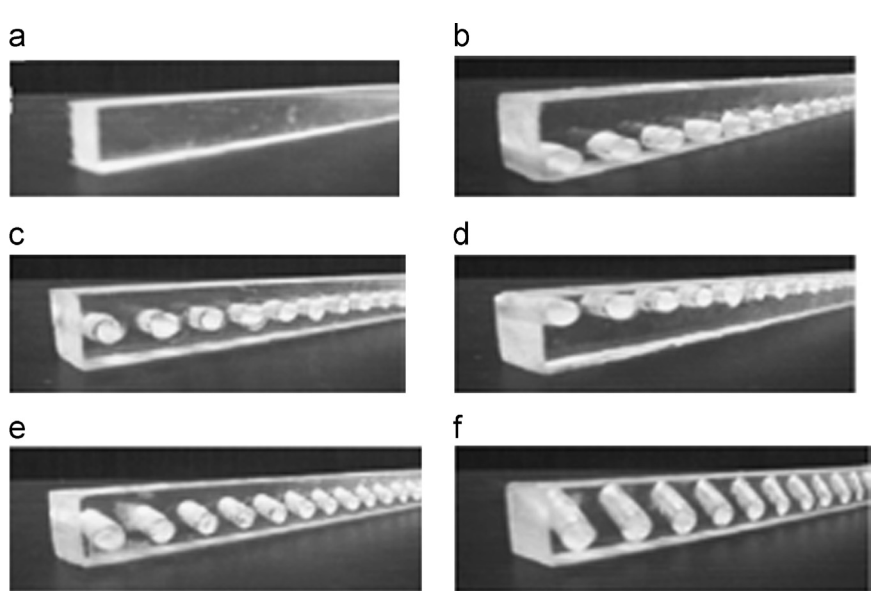


Fig. 12. Details of ribs geometry [49]. (a) Solid rib, (b) straight perforated rib (h=0.2H), (c) straight perforated rib (h=0.5H), (d) straight perforated rib (h=0.8H), (e) inclined perforated rib (θ=15°) and (f) inclined perforated rib (θ=30°).

friction factor and thermal performance enhancement factor for the in-phase 45° Z-baffles were found to be considerably higher than those for the out-phase 45° Z-baffle at a similar operating condition.

3.2. *Perforated ribs/blocks/baffles used in air duct*

As discussed earlier roughness elements of large height result in increase of heat transfer with more pressure drop penalty. Hot zones are also developed just downstream of ribs as a result of flow separation and recirculation around this position. This may lead to lower heat transfer. To overcome this problem efforts have been made to accelerate flow by providing perforations in the blockages. The perforation elements allow a part of flow to pass through perforation and thus hot zones are reduced.

Hwang and Liou [44] examined the effect of perforation ribs on heat transfer and friction factor in a channel. The experiment encompassed the Reynolds number (Re) ranging from 10,000 to 50,000, rib pitch-to-height ratio (PR) from 5 to 20 and rib height-to-channel hydraulic diameter ratio (H/D_h) from 0.081 to 0.162. The results indicated that perforated ribs had advantages of eliminating the hot spot and providing better heat transfer performance. Hwang et al. [45] further investigated heat transfer in a channel with perforated fences for three different types of turbulence promoters, namely solid, perforated and slit having half and fully perforated fences with open area ratios of 0, 10%, 22%, 38% and 44%. The major findings of the study were obtained as (i) local heat transfer deterioration that occurred just behind the solid fence channel was removed, (ii) thermal performance of the permeable-fenced channel was found better than as compared to channel with solid-fence, and (iii) the fence permeability was found to be the function of open area ratio and flow Reynolds number. Based on the finding, perforated fences of smaller thickness to height ratio were recommended in order to reduce the material requirements.

Sara et al. [46] investigated the thermal performance of a channel having a flat surface with solid and perforated rectangular blocks. Results were compared with those of similar channels without blocks. Energy gain upto 20% was found to be achieved by using perforated block. It was also found that heat transfer enhancement strongly depends upon perforation diameter, perforated area ratio, and inclination of perforation holes towards the surface of plate. Sara et al. [47] further investigated that the thermal performance of a similar channel flow provided perforated rectangular cross-sectional blocks attached on its surface for wide range of parameters. Reynolds number as 6670–40,000, the

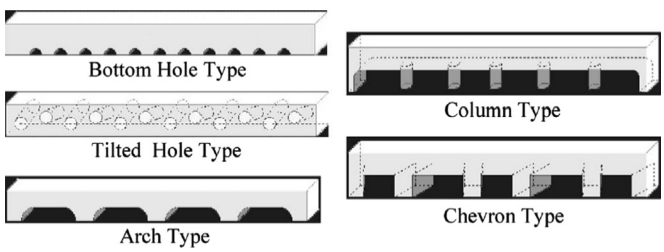


Fig. 13. Schematic of perforated ribs investigated in [50].

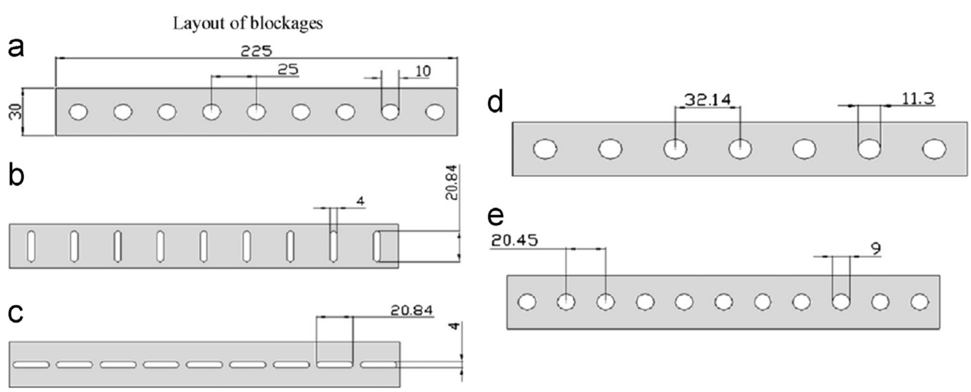


Fig. 14. Configuration of hole [51]. (a) Circular holes, (b) narrow holes, (c) wide holes, (d) circular 7 holes and (e) circular 11 holes.

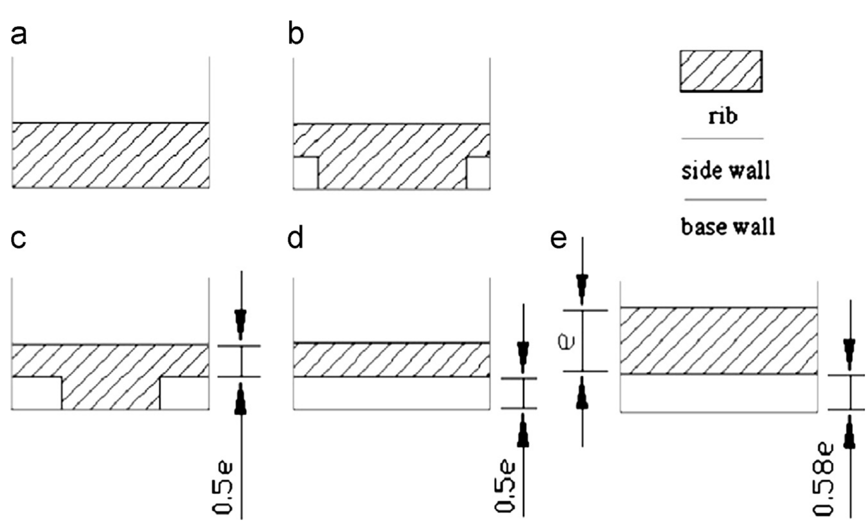


Fig. 15. Span wise shapes of five ribs [53]. (a) r/W=0, (b) r/W=0.125, (c) r/W=0.25, (d) r/W=0.5 and (e) detached.

hole inclination as 0–45°, perforation open area ratio as 0.05–0.15, diameter of perforation of 2.5–8.0 mm, number of blocks 2–7, ratio of pitch to hydraulic diameter 0.309–1.407. A better thermal efficiency has been found in a channel having blocks with inclined perforation. Further air channel provided with densely space blocks are found to have better thermal efficiency, moreover the pressure drops in terms of friction factor due to perforated blocks are found to be decreased in comparison to those of solid blocks.

Moon and Lau [48] studied heat transfer and pressure drop between two blockages with hole in a flow channel covering Reynolds number ranging from 10,000 to 30,000. Blockages in flow channel result an enhancement of 4.6–8.1 in heat transfer. However a significant increase of pressure drop has been observed. Nuntadusit et al. [49] investigated heat transfer and flow characteristics using LCT in a channel with six types of transverse perforated ribs as shown in Fig. 12. Perforation inclination angle ($\theta=0°$, 15°, 30°), location of hole on the rib ($h=0.2$ H, 0.5 H, 0.8 H) were considered as the important parameters. It was found that heat transfer immediately behind the rib was increased by decreasing the height of perforation hole. Further heat transfer was found to be increased with inclined perforation angles of ribs ($\theta=15°$, 30°) immediately behind the rib.

Shapes of holes affect the heat transfer and friction characteristics. Five different types of hole shapes made in Plexiglas as shown in Fig. 13 were investigated by Bucnhlin [50]. A ribs combination having pitch ratio of 5 with open area ratio as 0.53 has been found to be an efficient geometry for heat transfer.

Shin and Kwak [51] studied the effect of hole shape of blockages wall on heat transfer in a flow passage. Five shapes of hole narrow, wide and circular as shown in Fig. 14 were tested. It was observed that blockage wall with wider holes provided more uniform heat transfer coefficient and higher thermal performance factor. Liu and Chen [52] tested perforated and solid rectangular ribs detached from the wall in rectangular passage. It was observed that the thermal performance of detached solid-type ribs was found superior to that of perforated-type ribs. Liu and Wang [53] studied another five different structures of the ribs at two positions (45° and 90° angle of attack) as shown in Fig. 15. It was observed that semi-attached rib-design improved local heat transfer with semi-attached ribs with 45° angle of attack could produce a higher efficiency than that of the fully attached and detached rib channels.

Karwa et al. [54] investigated heat transfer and friction in rectangular ducts with perforated baffles attached on the heated surface for a range of Reynolds number from 2850 to 11,500. An increase of 82.7% in Nusselt number (Nu) was observed for duct with solid baffles when compared with smooth duct. However, Nusselt number (Nu) decreased from 62.9% to 49.7% when open area ratio (β) was increased from 18.4% to 46.8%. The friction factor for the solid baffles was found to be 11.1 times of the friction factor in smooth duct. Further it was observed that there was a significant decrease for the perforated baffles. Karwa and Maheshwari [55] investigated the fully and half perforated baffles (Fig. 16) covering the Reynolds number ranging from 2700 to 11,150. Maximum enhancement in the Nusselt numbers for fully perforated and half perforated were found to be 169% and 274% respectively. Half perforated baffles having relative pitch of 7.2 were found to have maximum enhancement in performance about 75% over a smooth duct for equal pumping power.

Liu et al. [56] studied impingement heat transfer on grooved surfaces geometry as shown in Fig. 17. These grooves were aligned either with the jet holes (inline pattern) or between the jet holes (staggered pattern). They used jet-to-target plate spacing (Z/d) as 3 and for a range the average jet Reynolds numbers ranging 2500–7700. Heat transfer was found to be increased near to grooves and there was no significant difference in overall averaged Nusselt numbers. A maximum enhancement of 15% was found to be with grooved surfaces.

A summary of important features of studies of various investigators are given in Table 1 for ready reference.

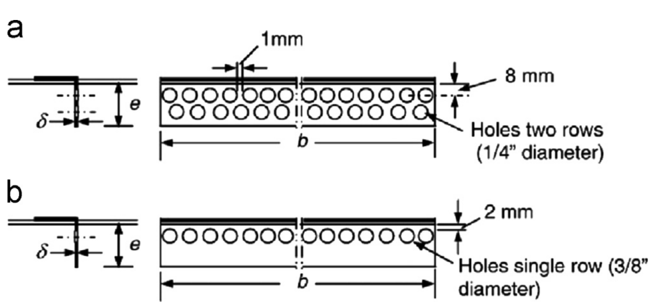


Fig. 16. Half perforated and fully perforated baffles [55].

3.3. Obstacles used in air heater duct

The purpose of introducing obstacles in the air duct is to create secondary flow, rotary flow or swirl/vortex turbulence, so as to increase the heat transfer coefficient and hence performance of air duct. Various shaped obstacles including vortex generators, delta shaped winglets, rectangular shaped winglets, rings, twisted tapes, cans which can be attached and bend out of plate so that they can create turbulence in the flow field, which results to enhance the heat transfer.

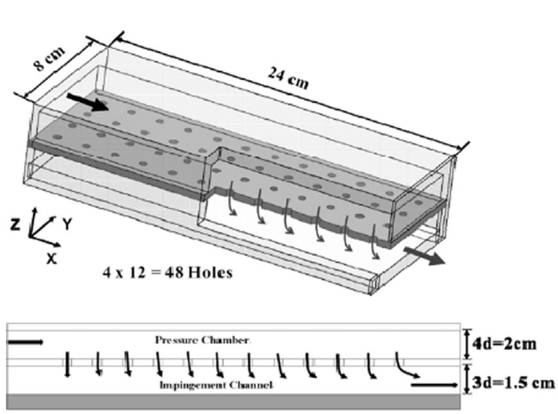


Fig. 2. Drawings of the impingement test section.

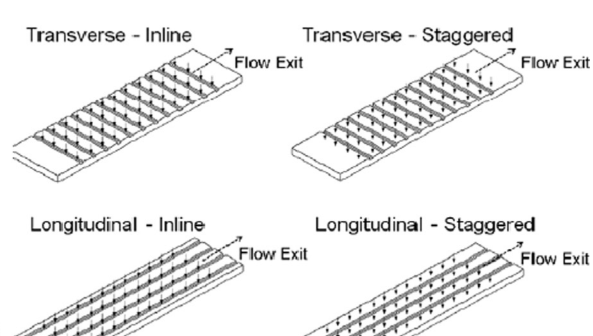


Fig. 17. Groove configuration on target surface [56].

Table 1
Summary of important feature of perforated baffles/blockages used by various investigators.

S. No.	Investigators	Type of ribs and arrangement	Reynolds number (Re)	Aspect ratio (W/H)	Relative roughness height (e/D_h)	Relative roughness pitch (p/e)	Relative thickness (t/e)	Perforation angle (φ)	Open area ratio (β)	Correlations	Remark
1	Hwang and Liou [44]	Solid and perforated ribs on two opposite walls in staggered fashion	1×10^4–5×10^4	4.0	0.081, 0.162	5, 10, 15 and 20	$t=4$ mm	0°	0 and 50%	$\mathrm{Re}=3.31(PR/10)^{0.53}$ $G=3.72(H^+)^{0.35}(PR/10)^{0.08}$ for solid rib $\mathrm{Re}=5.15(PR/10)^{0.53}$ $G=2.25(H^+)^{0.35}(PR/10)^{0.08}$ for perforated rib	$\mathrm{Nu}/\mathrm{Nu}_s^*=1.0-1.55$ for solid and 1.15 for perforated, f/f_s=6–9 for solid and 4–6 for perforated
2	Hwang et al. [45]	Perforated fences on two opposite walls	8000–5×10^4	4.0	0.081	10	0.16–0.7	0°	0, 10%, 22%, 38%, 44%	$Nu=0.335\mathrm{Re}^{0.624}$ $f=0.00451\beta^{-0.106}$	Perforated fences for small t/e give better performance
3	Sara et al. [46]	Perforated block attached to one wall	6670–4×10^4	2.0	0.081	0.309–1.407	0.4	0°–45°	0.04–0.15	$\overline{Nu}/Nu_s=19.586\mathrm{Re}^{-0.186}(S_x/D_e)^{0.05}(D/D_e)^{0.05}\beta^{0.10}(1/\cos\theta)^{0.17}$ $f=7.074\mathrm{Re}^{-0.277}(S_x/D_e)^{-0.036}(D/D_e)^{-0.06}\beta^{-0.066}$	$\mathrm{Nu}/\mathrm{Nu}_s^*$=0.8–1.0 for solid and 1.0–1.4 for perforated, f/f_s=0.7–0.9 for solid and 0.3–0.8 for perforated
4	Liou and Chan [52]	Solid and perforated ribs detached from wall	5000–5×10^4	4.0	0.081, 0.106, 0.162	10	$t=5.2$ mm	0°	4%	$\overline{Nu}/Nu_s=30.04Re^{-0.2}(e/D_e)^{0.31}$ $f=7.074Re^{-0.046}(e/D_e)^{0.47}$ For detached perforated ribs	Detached solid and perforated ribs are better than detached perforated ribs
5	Moon and Lau [48]	Perforation in middle, above mid-plane and below mid-plane in blockage of duct size	2×10^4–3×10^4	5.84	1	$p=63.5$ and 76.2 mm	$t=19.1$ mm	0°	16.33% and 36.94%	–	Nu=155.79–244.75, f=5.34–42.79 For Re 2×10^4 Nu=320.08–501.39, f=5.08–47.26 For Re 3×10^4
6	Liu and Wang [53]	Semi-attached, detached and solid rib at angle of attack 45°, 90°	1×10^4–2.5×10^4	2.42	0.25	$p=40$ mm	1.0	45°,0°	0, 0.125, 0.25, 0.5, 0.58	–	Rib with 0.125% open area ration have highest performance at 45° angle of attack
7	Karwa and Maheswari [55]	Half and fully perforated baffles	2700–11,150	7.77	0.495	$P=137$, 274, 548 mm	0.047	0°	7.21%, 14.42%, 26%, 28.84%, 46.8%,	$Nu=0.893\mathrm{Re}^{0.78608}$ $f=0.1673\mathrm{Re}^{-0.0213}$ for half perforated baffles with 26% open area ratio	Half perforated baffles with 26% open area ration have 51.6%–75% over smooth duct at equal pumping power.
8	Karwa et al. [54]	Perforated baffles	2850–11,500	7.77	0.495	$P=550$ mm	0.047	0°	18.4%, 28.4%, 41.7%, 46.8%	–	Baffles with 46.8% open area ratio have best performance compared to smooth duct at equal pumping power.
9	Shin and kwak [51]	Perforated blocks with five different hole shapes	2×10^4–4×10^4	7.5	1.0	–	–	0°	–	–	Wide hole have high Nusselt number compare to other. Rib have open area ratio 20% being optimum
10	Nuntadusit et al. [49]	Perforation on block at different heights and angles	60×10^4	4.0	0.3	–	0.67	0°, 15° and 30°	10%, 20%, 30%, 40%, 50%	–	Perforated rib with small h/H ratio shows superior improvement of heat transfer
11	Tariq et al. [36]	Rib with slit perforation	4000, 32,100	1.86	0.0624	0.0624	–	0°	10%, 20%, 30%, 40%, 50%	–	Rib have open area ratio 20% being optimum

Gentry et al. [57] enhanced average heat 50%–60% for flow over a flat plate at low Reynolds numbers, using delta-wing vortex generators. They used optimal delta-wing geometries for Reynolds numbers of 600, 800 and 1000 based on wing-chord length. Torii et al. [58] investigated two types of arrangement (staggered and in-line) of delta winglet-type vortex generators in a fin-tube heat exchanger as shown in Fig. 18. The heat transfer was augmented by 10%–30% in case of staggered arrangement, and yet the pressure loss was reduced by 55%–34%. But, in case of in-line tube arrangement, these were found to be 10%–20% augmentation and 15%–8% reduction in pressure. Min et al. [59] studied fluid flow and heat transfer characteristics of longitudinal vortex generator (LVG) mounted in rectangular channel as shown in Fig. 19. It was concluded that local heat transfer had been enhanced due to strong longitudinal vortices generated by the presence on the LVGs near the positions of $z = \pm 40$ mm from the centreline of the heater plate. The down-sweep of the longitudinal vortices was beneficial to the heat transfer enhancement.

Zhou and Ye [60] investigated the thermohydraulic performance of curved trapezoidal winglet as shown in Fig. 20. Results were compared with rectangular winglet, trapezoidal winglet and delta winglet. It was observed that curved trapezoidal winglet delta winglet had the best thermohydraulic performance in fully turbulent flow region. However, delta winglet had the best in laminar and transitional flow region. Kotcioglu et al. [61] investigated the second law of a cross-flow heat exchanger duct having winglets in the presence of a balance between the entropy generations. It was concluded that increasing the cross-flow fluid velocity enhances the heat transfer rate and reduces the heat transfer irreversibility. Geometry and placement of winglets in rectangular channel are shown in Fig. 21.

Promvonge et al. [62] studied the effects of combined ribs and delta-winglet type vortex generators (DWs) for turbulent airflow through air heater duct as shown in Fig. 22. Ten pairs of the DWs having roughness height 0.4 were tested with transverse pitch ration 1 and three attack angles of 60°, 45° and 30°. It was concluded that Nusselt number and friction factor values for combined rib and DWs, found to be much higher than those for the rib/DW alone. Chompookham et al. [63] also studied the effect of combined wedge ribs and winglet type vortex generators (WVGs) on heat transfer and friction loss characteristics. Both wedge ribs and WVGs arranged on the opposite channel walls were staggered and in-line arrays. Due to combined ribs and the WVGs, significant increment in heat transfer rate and friction loss over the smooth channel was observed. The winglet geometry is shown in Fig. 23.

Bekele et al. [64] investigated the effect of delta-shaped obstacles in solar air heater duct as shown in Fig. 24. Longitudinal pitch (Pl/e) and relative obstacle height (e/H) were the main parameters and varied from 3/2 to 11/2 and 0.25 to 0.75 respectively. These obstacle-mounted duct enhanced the heat transfer by 3.6-times over smooth duct under similar geometrical and flow conditions at Re=7276.82, $Pl/e = 3/2$, and $e/H = 0.75$. Abene et al. [65] also studied the effect of obstacles in air duct. The different

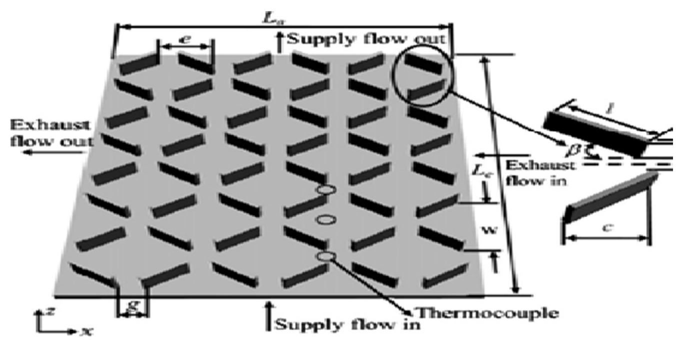


Fig. 21. Placement of winglets in rectangular channel [61].

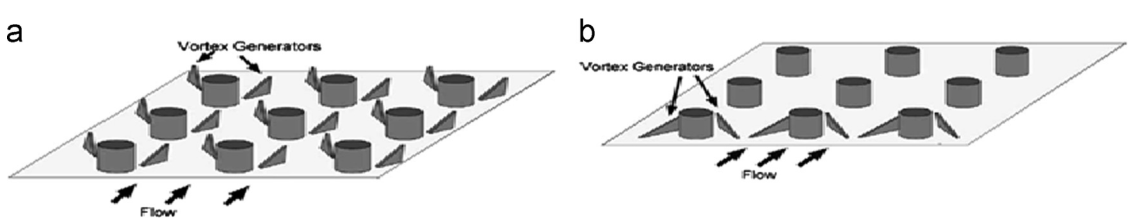


Fig. 18. Configuration of winglet type vortex on the surface-tube bank: (a) “common flow down” configuration; and (b) “common flow up” configuration [58].

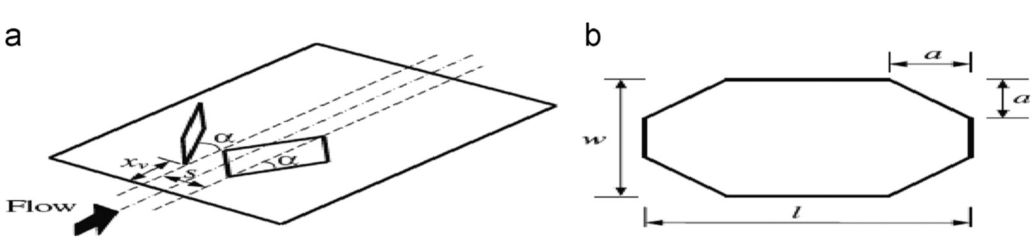


Fig. 19. Schematic view of present modified longitudinal vortex generator: (a) layout of common-flow-down wings and (b) modified rectangular wing [59].

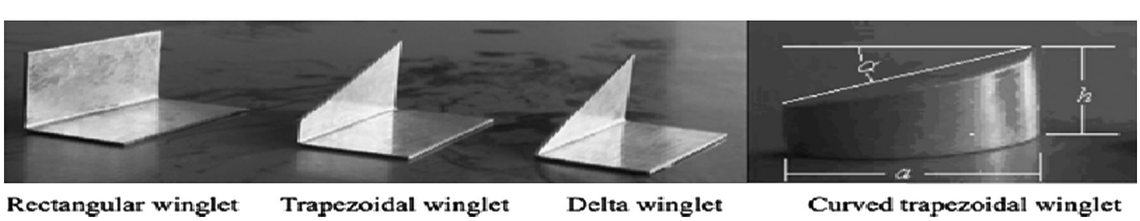


Fig. 20. Winglets [60].

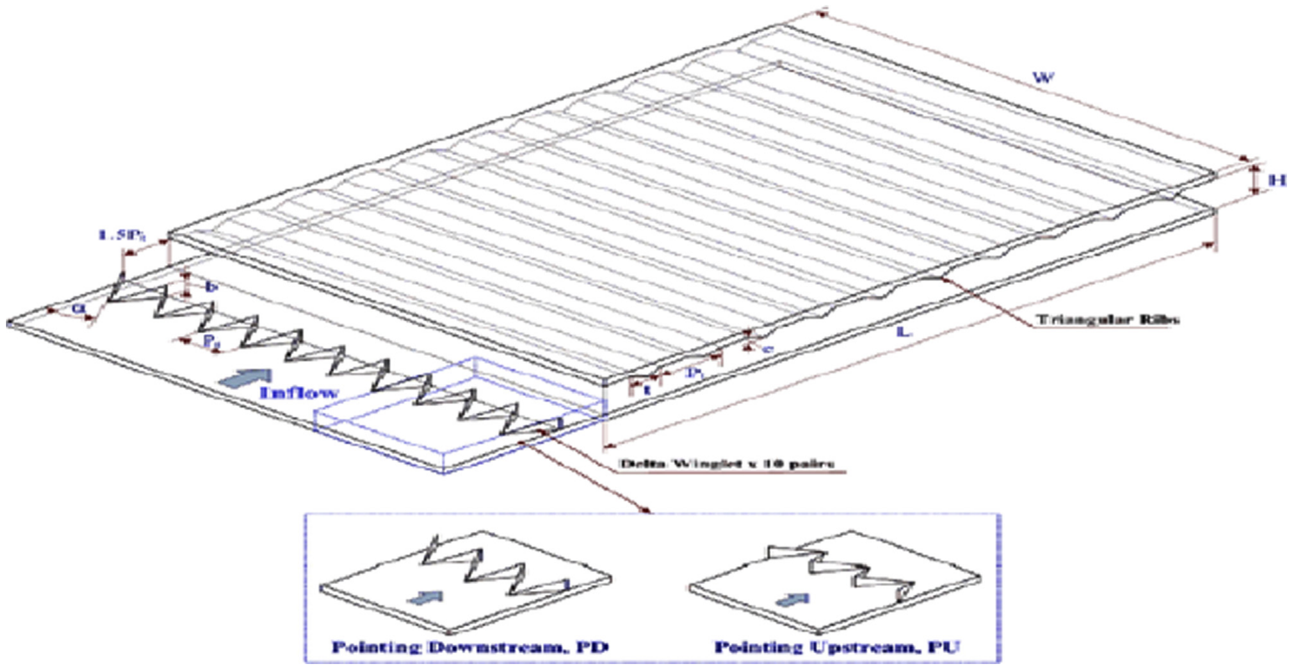


Fig. 22. Test sections with pointing downstream and pointing upstream [62].

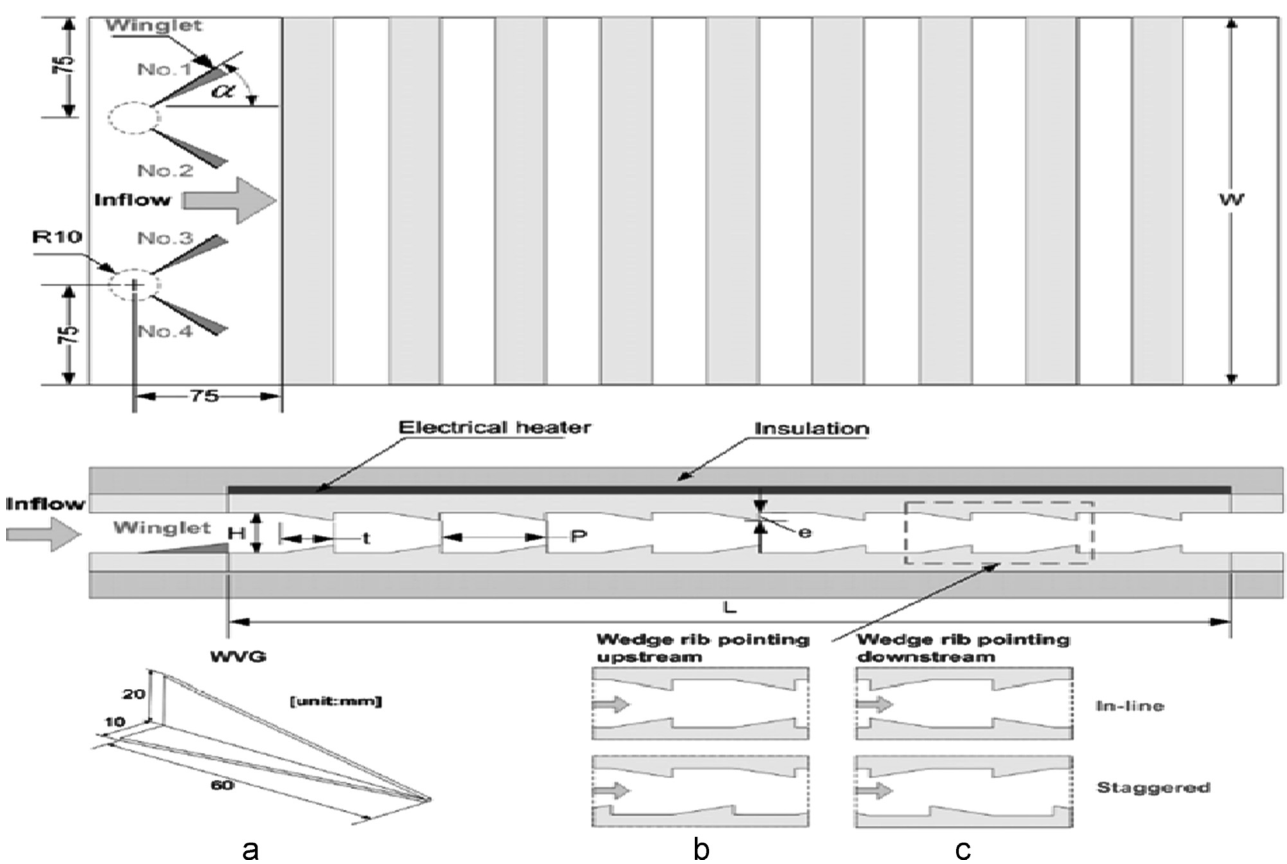


Fig. 23. Test section with (a) winglet geometry; (b) wedge rib pointing upstream; and (c) wedge rib pointing downstream [63].

shapes studied, were ogival transverse (OT), ogival inclined folded (OIF), waisted tube (WT), waisted delta lengthways (WDLs), waisted ogival lengthways (WOLs) and transverse longitudinal obstacles (TL) as shown in Fig. 25. It was observed that the form, dimensions, orientation and disposition of the obstacles strongly influences the collector efficiency. Esen [66] presented an experimental energy and exergy analysis for a solar air heater with several obstacles and without obstacles. The results demonstrate that optimal values of efficiency were middle level of absorbing plate in flow channel duct and the double-flow collector supplied with obstacles appears significantly better than that without obstacles.

Ozgen et al. [67] investigated obstacles in the form of aluminium cans in the double-pass channel of a flat-plate solar air heater. Two different arrangements of cans namely staggered and regular on absorber plates were employed for experiment. Staggered arrangement was found to be the best. Arrangements of cans on the absorber plate are shown in Fig. 26.

Nguyen et al. [68] numerically studied fluid flow and heat transfer in circular tubes within internal circumferential rib. It was reported that the ratio of thermal conductivity of wall to that of fluid affected heat transfer and enhancement in heat transfer was found for high Prandlt number (Pr) fluids in roughened tube. Gee and Webb [69] investigated the heat transfer and friction

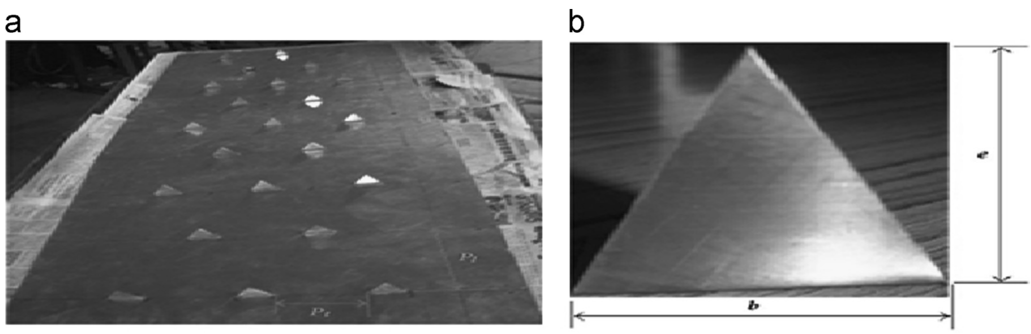


Fig. 24. Delta shaped obstacles mounted on plate [64].

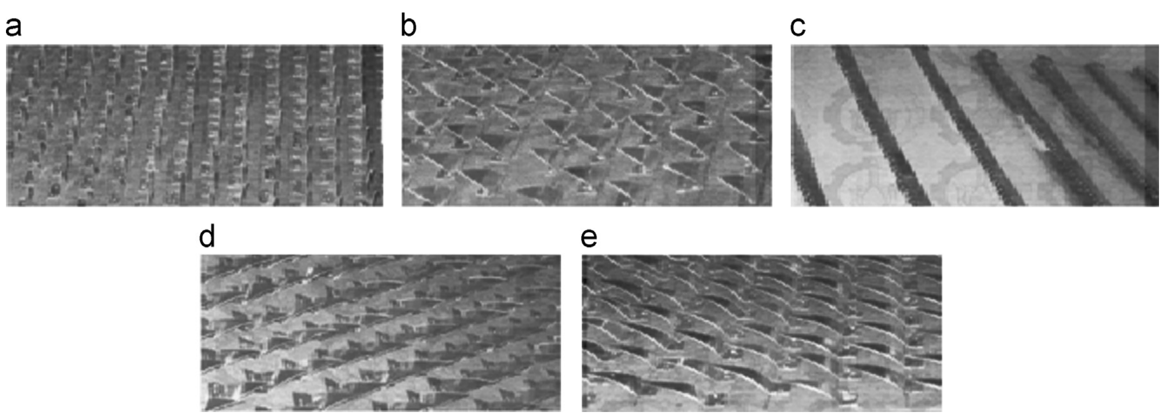


Fig. 25. Different obstacles geometry: (a) OT; (b) OIF1; (c) WT; (d) WDL1; and (e) WOL1 [65].

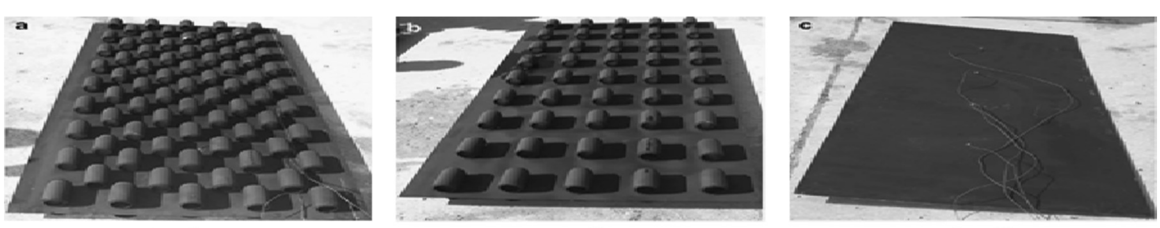


Fig. 26. Aluminums cans attached on absorber plate [67].

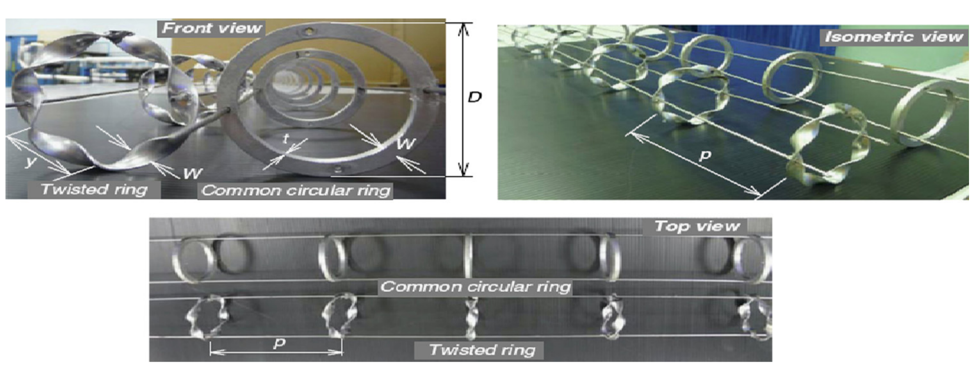


Fig. 27. Twisted ring studied by Thianpong [70].

factor characteristics of helical-rib surface in circular tube. Three different helix angles (30°, 49° and 70°) were considered to design the helical-rib. It was observed that helical-rib with helix angle of 49° provided the highest performance.

Thianpong et al. [70] investigated heat transfer, friction factor and thermal performance characteristics of a tube equipped with twisted rings (TRs). Three distinct rings were tested as shown in Fig. 27. It was concluded that in comparison to common circular rings (CRs), twisted rings (CRs) gave lower Nusselt number (Nu) and friction factor (f), except at the largest width ratio ($W/D=0.15$) and the smallest pitch ratio ($p/D=1.0$). Further, maximum thermal performance factor had been found corresponding to smaller value of width ratio and pitch ratio. Eiams-ard et al. [71] performed the experiments to find out effects of the typical twisted tape (TT), oblique delta-winglet twisted tape (O-DWT) and straight delta-winglet twisted tape (S-DWT) arrangements in a tube as shown in Fig. 28. It was observed that Nusselt number, friction factor and thermal performance factor in a tube with the O-DWT were, respectively, 1.04–1.64, 1.09–1.95, and 1.05–1.13 times of those in the tube with TT.

Smith et al. [72] investigated the effects of tandem wire coil elements in the form of turbulators (Fig. 29) on heat transfer and turbulent flow friction characteristics in a uniform heat-flux square duct. Full-length coil, 1D and 2D length coil elements were placed in tandem inside the duct with various free-space lengths to reduce the friction loss. It was observed that Nusselt number and friction ratio of tandem wire coil elements with that of smooth duct were found in the range of 1.7–2.45 and 4.5–9.5 respectively.

Summary of distinct turbulators studied by various investigators are given in Table 2.

4. Conclusions

An attempt has been made to review heat transfer and friction characteristics of roughened ducts provided with turbulators. Based on the literature it is found that perforated baffles are considered to be thermo-hydraulically better in comparison to solid baffles because perforation in ribs/blocks/baffles enhances

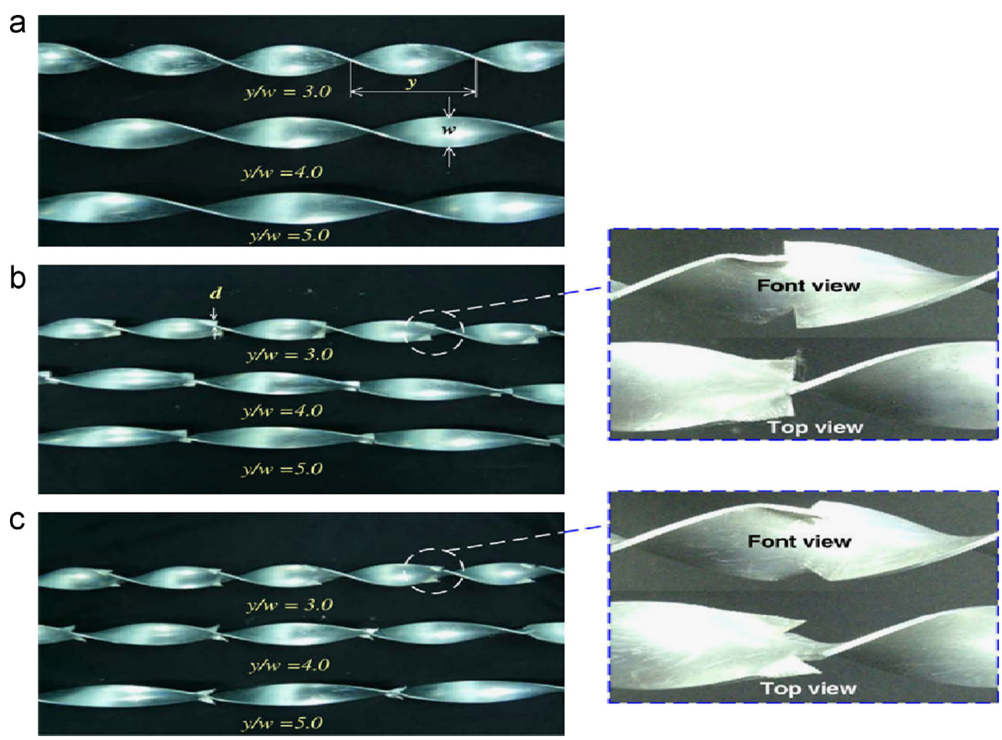


Fig. 28. Twisted tape vortex generator: (a) typical twisted type (TT); (b) straight-delta winglet twisted t types (S-DWT); and (c) oblique-delta winglet twisted (O-DWT) [71].

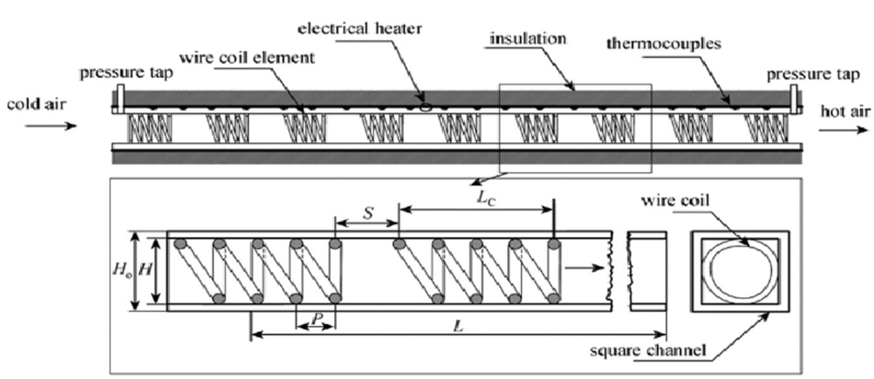


Fig. 29. Test duct fitted with wire coil elements [72].

Table 2
Summary of important features of turbulators used by various investigators.

S. No.	Author	Arrangement	Reynolds number (Re)	Angle of attack (α)	Relative height (e/D or e/D_h)	Relative pitch (P/e)	Other parameter	Correlation	Remark
1	Eiamsa-ard et al. [71]	Typical twisted type (TT), Straight-Delta winglet twisted t types (S-DWT), Oblique- Delta winglet twisted (O-DWT)	30,002,700	——	Circular pipe	–	Twist ratios (y/w)=3, 4 and 5, Wing cut ratios (d/w)=0.11, 0.21 and 0.32	For O-DWT $f=24.8\mathrm{Re}^{-0.51}(y/w)^{-0.556}(1+d/w)^{1.87}$ $\eta=2.04\mathrm{Re}^{-0.042}\mathrm{Pr}^{0.4}(y/w)^{-0.261}(1+d/w)^{0.45}$ For S-DWT QUOTE QUOTE $Nu=0.184\mathrm{Re}^{0.675}\mathrm{Pr}^{0.4}(y/w)^{-0.465}(1+d/w)^{0.76}$ $f=21.7\mathrm{Re}^{-0.45}(y/w)^{-0.564}(1+d/w)^{1.41}$ $\eta=2.164\mathrm{Re}^{-0.0435}\mathrm{Pr}^{0.4}(y/w)^{-0.304}(1+d/w)^{0.346}$	Ration of Nusselt number, friction factor, thermal performance factor of O-DWT to S-DWT. Respectively 1.04–1.64, 1.09–1.95, 1.05–1.13
2	Min et al. [59]	Modified rectangular longitudinal vortex generators	5000–17,500	$\alpha=25°–65°$	–	–	$W/H=4$	———	$\mathrm{Nu}_{max}=170$, at $\alpha=55°$
3	Sriromreun [43]	Z-shaped baffles	4400–20,400	$\alpha=45°$	$e/H=0.1–0.3$	$P/H=1.5–3$	$W/H=10$	———	$\mathrm{Nu}_{max}=380$ and f_{max}1.1 at $e/H=0.3$, $P/H=1.5$, in phase
4	Eiamsa-ard et al. [68]	Wire coil element insert	4000–25,000	–	–	–	Free space ratio (S/D)=1–5,	———	$(\mathrm{Nu}/\mathrm{Nu}_s)_{max}=1.7–2.45$, $(f/f_s)_{max}=4.9–9.5$
5	Thianpong et al. [70]	Twisted rings turbulators	4000–20,000	–	–	Pitch ratio (P/D)=1–2	Width ratio (W/D)=0.05–0.15	$Nu=0.097\mathrm{Re}^{0.833}\mathrm{Pr}^{0.4}(W/D)^{0.408}(p/D)^{-0.181}$ $f=112.795\mathrm{Re}^{-0.159}(W/D)^{1.665}(p/D)^{-0.736}$	Maximum performance factor=1.24 is at $W/D=0.05$ and $p/D=1.0$ at a Reynolds number of 6000.
6	Liu et al. [56]	Jet impingement of jet on groove surface	2500–7000	–	–	–	Jet-to-target plate spacing (Z/d)=3	–	For both transverse and longitudinal grooves, the staggered arrangement with respect to the jet arrays gave higher Nusselt number.
7	Torri et al. [58]	Winglet-type vortex generators	350–2100	–	–	–	In-line arrangement and staggered arrangement	–	In case of staggered tube banks ,the heat transfer was augmented by 30% to 10%, with the winglet pairs of the present configuration, In case of in-line tube banks, the heat transfer was augmented by 20% to 10%.
8	Chompookham et al. [63]	Winglet-type vortex generators	5000–22,000	$\alpha=60°$	$e/H=0.2$	$P/H=1.33$	wedge rib pointing upstream, wedge rib pointing downstream.	–	Combination of staggered wedge rib and the WVGs performed efficiently.
9	Promvonge et al. [62]	Rib with delta winglet	5000–20,000	$\alpha=30°–60°$	$e/H=0.2$,	$P/H=1.33$	Delta winglet arrangement (a) pointing upstream, (b) pointing downstream	——	Heat transfer augmentation $\mathrm{Nu}/\mathrm{Nu}_s=2.3–2.6$, pressure drop ratio f/f_s-4.7–10.1
10	Zhou et al.[60]	Trapezoidal winglet type vortex generators	700–26,800	$\alpha=0°–90°$	$h/H=0.5$	–	Length of vortex generator (a)=40, Width of vortex generator (b)=0–20	–	Smaller attack angle, larger curvature and larger angle of inclination gives better thermohydraulic performance
11	Bekele et al. [64]	Delta shaped obstacles	3400–27,600	$\alpha=90°$	$e/H=0.25–0.75$	Longitudinal pitch (P_l/e)=3/2–11/2	Relative obstacle transversal pitch (P_t/b)=7/3	–	$\mathrm{Nu}/\mathrm{Nu}_s=3.6$ at Re=7276.82,$P_l/e=3/2$, and $e/H=0.75$.
12	Esen [66]	Obstacles on both side of absorber plate	Mass flow rate (m)=0.015–0.2 kg/s	–	–	–	–	–	The mean efficiencies for Type I, Type II, Type III, and Type IV were found to be 38%, 43%, 45%, and 41%, respectively.

the heat transfer due to elimination of hot spot just behind the ribs.

Shape of hole and inclination of perforation are considered the main parameters which affect the heat transfer and friction characteristics of air duct. Turbulators in the form of winglets, rings, twisted rings, Z shaped baffles vortex generator, obstacles and winglet were used in air heaters and found suitable to create turbulence to increase the heat transfer rate; however, substantial increase in pressure drop has been observed. Therefore, the design of the vortex generator is found to be a very critical task which needs attention to minimise the pressure drop through ducts. The compound delta winglets having perforations can be used to enhance heat transfer with minimum pressure drop for overall performance enhancement of solar air heater duct.

References

[1] Nikuradse J. Laws of flow in rough pipes. NACA technical memorandum; 1958, p. 1292.
[2] Dippery DF, Sabersky RH. Heat and momentum transfer in smooth and rough tubes at various prandlt numbers. Int J Heat Mass Transf 1963;6:329–53.
[3] Gomelauri V. Influence of two-dimensional artificial roughness on convective heat transfer. Int J Heat Mass Transf 1964;7:653–63.
[4] Kolar V. Heat transfer in turbulent flow of fluids through smooth and rough tubes. Int J Heat Mass Transf 1965;8:639–53.
[5] Sheriff N, Gumley P. Heat transfer and friction properties of surfaces with discrete roughnesses. Int J Heat Mass Transf 1966;9:1297–320.
[6] Webb RL, Eckert ERG, Goldstein RJ. Heat transfer and friction in tubes with repeated-rib roughness. Int J Heat Mass Transf 1971;14:601–17.
[7] Webb RL, Eckert ERG, Goldstein RJ. Generalized heat transfer and friction correlations for tubes with reapeted-rib roughness. Int J Heat Mass Transf 1972;15:180–4.
[8] Webb RL, Eckert ERG. Application of rough surfaces to heat exchanger design. Int J Heat Mass Transf 1972;15:1647–58.
[9] Donne MD, Meyer L. Turbulent convective heat transfer from rough surfaces with two-dimensional rectangular ribs. Int J Heat Mass 1977;20:583–620.
[10] Bergles A, Webb R, Junkan G. Energy conservation via heat transfer enhancement. Energy 1979;4:193–200.
[11] Das MK, Tariq A, Panigrahi PK, Muralidhar K. Estimation of convective heat transfer coefficient from transient liquid crystal data using an inverse technique. Inverse Probl Sci Eng 2005;13:133–55.
[12] Han JC, Ou S, Park JS, Lei CI. Augmenter heat transfer in rectangular channels of narrow aspect ratios with rib turbulators. Int J Heat Mass 1989;32:1619–30.
[13] Han JC, Glicksman LR, Rohsenow WM. An investigation of heat transfer and friction for rib-roughened surfaces. Int J Heat Mass Transf 1978;21:1143–56.
[14] Firth R, Meyer L. A comparison of the heat transfer of four different types of artificially roughened surface. Int J Heat Mass 1983;26:175–83.
[15] Han JC, Park JS. Developing heat transfer in rectangular channels with rib turbulators. Int J Heat Mass Transf 1988;31:183–95.
[16] Han J. Heat transfer and friction characteristics in rectangular channels with rib turbulators. ASME J Heat Transf 1988;110:321–8.
[17] Park JS, Han JC, Huang Y, Ou S. Heat transfer performance comparisons of five different rectangular channels with parallel angled ribs. Int J Heat Mass 1992;35:2891–903.
[18] Hong YJ, Hsieh SS. An experimental investigation of heat transfer characteristics for turbulent flow over staggered ribs in a square duct. Exp Therm Fluid Sci 1991;4:714–22.
[19] Facchini B, Innocenti L, Surace M. Design criteria for ribbed channels: experimental investigation and theoretical analysis. Int J Heat Mass Transf 2006;49:3130–41.
[20] Khan RK, Ali MAT, Akhanda MAR. Heat transfer augmentation in developing flow through a ribbed square duct. J Therm Sci 2006;15:251–6.
[21] Liu J, Gao J, Gao T, Shi X. Heat transfer characteristics in steam-cooled rectangular channels with two opposite rib-roughened walls. Appl Therm Eng 2013;50:104–11.
[22] Liou TM, Hwang JJ. Effect of ridge shapes on turbulent heat transfer and friction in a rectangular channel. Int J Heat Mass 1993;36:931–40.
[23] Sparrow E, Charmchi M. Heat transfer and fluid flow characteristics of spanwise-periodic corrugated ducts. Int J Heat Mass Transf 1980;23:471–81.
[24] Sparrow EM, Hossfeld LM. Effect of rounding of protruding edges on heat transfer and pressure drop in a duct. Int J Heat Mass Transf 1984;27:1715–23.
[25] Sara ON, Pekdemir T, Yapmcm S, Ymlmaz M. Enhancement of heat transfer from a flat surface in a channel flow by attachment of rectangular blocks. Int J Energy Res 2001;25:563–76.
[26] Won SY, Burgess NK, Peddicord S, Ligrani PM. Spatially resolved surface heat transfer for parallel rib turbulators with 45 deg orientations including test surface conduction analysis. J Heat Transf 2004;126:193–201.
[27] Tanda G. Heat transfer in rectangular channels with transverse and V-shaped broken ribs. Int J Heat Mass Transf 2004;47:229–43.
[28] Wang L, Sunden B. An experimental investigation of heat transfer and fluid flow in a rectangular duct with broken V-shaped ribs. Exp Heat Transf 2004;17:243–59.
[29] Wang L, Sundén B. Experimental investigation of local heat transfer in a square duct with various-shaped ribs. Heat Mass Transf 2006;43:759–66.
[30] Gupta A, SriHarsha V, Prabhu SV, Vedula RP. Local heat transfer distribution in a square channel with 90° continuous, 90° saw tooth profiled and 60° broken ribs. Exp Therm Fluid Sci 2008;32:997–1010.
[31] Maurer M, Jens VW, Gritisch M. An experimental and numerical study of heat transfer and pressure losses of V and W shaped ribs at high Reynolds number. Proc ASME Turbo Expo 2007;4:219–28.
[32] Lesley MW, Fu WL, Han JC. Thermal performance of angled, V-Shaped, and W-Shaped rib turbulators in rotating rectangular cooling channels (AR=4:1). J Turbomach 2004;126:604–14.
[33] Lau SC, Kukreja RT, Mcmillin RD. Effects of V-shaped rib arrays on turbulent heat transfer and friction of fully developed flow in a square channel. Int J Heat Mass Transf 1991;34:1605–16.
[34] Han JC, Zhang YM. High performance heat transfer ducts with parallel broken and V-shaped broken ribs. Int J Heat Mass Transf 1991;35:513–23.
[35] Smith CR, Sabatino DR, Praisner TJ. Temperature sensing with thermochromic liquid crystals. Exp Fluids 2001;30:190–201.
[36] Tariq A, Panigrahi PK, Muralidhar K. Flow and heat transfer in the wake of a surface-mounted rib with a slit. Exp Fluids 2004;37:701–19.
[37] Panigrahi PK, Schröder A, Kompenhans J. PIV investigation of flow behind surface mounted permeable ribs. Exp Fluids 2005;40:277–300.
[38] Chaube A, Sahoo PK, Solanki SC. Analysis of heat transfer augmentation and flow characteristics due to rib roughness over absorber plate of a solar air heater. Renew Energy 2006;31:317–31.
[39] Promvonge P, Thianpong C. Thermal performance assessment of turbulent channel flows over different shaped ribs. Int Commun Heat Mass Transf 2008;35:1327–34.
[40] Kamali R, Binesh R. The importance of rib shape effects on the local heat transfer and flow friction characteristics of square ducts with ribbed internal surfaces. Int Commun Heat Mass Transf 2008;35:1032–40.
[41] Yeh HM, Chou W. Efficiency of solar air heaters with baffles. Energy 1991;16:983–7.
[42] Promvonge P. Heat transfer and pressure drop in a channel with multiple 60° V-baffles. Int Commun Heat Mass Transf 2010;37:835–40.
[43] Sriromreun P, Thianpong C, Promvonge P. Experimental and numerical study on heat transfer enhancement in a channel with Z-shaped baffles. Int Commun Heat Mass Transf 2012;39:945–52.
[44] Hwang JJ, Liou TM. Heat transfer in a rectangular channel with perforated turbulence promoters using holographic interferometry measurement. Int J Heat Mass Transf 1995;38:3197–207.
[45] Hwang JJ, Lia TY, Liou TM. Effect of fence thickness on pressure drop and heat transfer in a perforated-fenced channel. Int J Heat Mass Transf 1998;41:811–6.
[46] Sara ON, Pekdemir T, Yapici S, Yilmaz M. Heat-transfer enhancement in a channel flow with perforated rectangular blocks. Heat Fluid Flow 2001;22:509–18.
[47] Sara ON, Pekdemir T, Ersahan H. Thermal performance analysis for solid and perforated blocks on a flat surface in a duct flow. Energy Convers Manag 2000;41:1019–28.
[48] Moon SW, Lau SC. Heat transfer between blockages with holes in a rectangular channel. J Heat Transf 2003;125:587.
[49] Nuntadusit C, Wae-hayee M, Bunyajitradulya a, Eiamsa-ard S. Thermal visualization on surface with transverse perforated ribs. Int Commun Heat Mass Transf 2012;39:634–9.
[50] Buchlin J. Convective heat transfer in a channel with perforated ribs Transfert de chaleur par convection dans un canal muni de pontets perforés. Therm Sci 2002;41:332–40.
[51] Shin S, Kwak JS. Effect of hole shape on the heat transfer in a rectangular duct with perforated blockage walls. J Mech Sci Technol 2008;22:1945–51.
[52] Liou T-M, Chen S-H. Turbulent heat and fluid flow in a passage disturbed by detached perforated ribs of different heights. Int J Heat Mass Transf 1998;41:1795–806.
[53] Liu H, Wang J. Numerical investigation on synthetical performances of fluid flow and heat transfer of semiattached rib-channels. Int J Heat Mass Transf 2011;54:575–83.
[54] Karwa R, Maheshwari BK, Karwa N. Experimental study of heat transfer enhancement in an asymmetrically heated rectangular duct with perforated baffles. Int Commun Heat Mass Transf 2005;32:275–84.
[55] Karwa R, Maheshwari BK. Heat transfer and friction in an asymmetrically heated rectangular duct with half and fully perforated baffles at different pitches. Int Commun Heat Mass Transf 2009;36:264–8.
[56] Liu YH, Song SJ, Lo YH. Jet impingement heat transfer on target surfaces with longitudinal and transverse grooves. Int J Heat Mass Transf 2013;58:292–9.
[57] Gentry MC, Jacobi AM. Heat transfer enhancement by delta-wing vortex generators on a flate plate: vortex interaction with the boundary layer. Exp Therm Fluid Sci 1997;14:231–42.
[58] Torii K, Kwak KM, Nishino K. Heat transfer enhancement accompanying pressure-loss reduction with winglet-type vortex generators for fin-tube heat exchangers. Int J Heat Mass Transf 2002;45:3795–801.
[59] Min C, Qi C, Kong X, Dong J. Experimental study of rectangular channel with modified rectangular longitudinal vortex generators. Int J Heat Mass Transf 2010;53:3023–9.

[60] Zhou G, Ye Q. Experimental investigations of thermal and flow characteristics of curved trapezoidal winglet type vortex generators. Appl Therm Eng 2012;37:241–8.
[61] Kotcioglu I, Caliskan S, Cansiz A, Baskaya S. Second law analysis and heat transfer in a cross-flow heat exchanger with a new winglet-type vortex generator. Energy 2010;35:3686–95.
[62] Promvonge P, Khanoknaiyakarn C, Kwankaomeng S, Thianpong C. Thermal behavior in solar air heater channel fitted with combined rib and delta-winglet. Int Commun Heat Mass Transf 2011;38:749–56.
[63] Chompookham T, Thianpong C, Kwankaomeng S, Promvonge P. Heat transfer augmentation in a wedge-ribbed channel using winglet vortex generators. Int Commun Heat Mass Transf 2010;37:163–9.
[64] Bekele A, Mishra M, Dutta S. Effects of delta-shaped obstacles on the thermal performance of solar air heater. Adv Mech Eng 2011;2011:1–10.
[65] Abene A, Dubois V, Le RM, Ouagued A. Study of a solar air flat plate collector: use of obstacles and application for the drying of grape. J Food Eng 2004;65:15–22.
[66] Esen H. Experimental energy and exergy analysis of a double-flow solar air heater having different obstacles on absorber plates. Build Environ 2008;43:1046–54.
[67] Ozgen F, Esen M, Esen H. Experimental investigation of thermal performance of a double-flow solar air heater having aluminium cans. Renew Energy 2009;34:2391–8.
[68] Nguyen TM, Khodadadi JM, Vlachos NS. Laminar flow and conjugate heat transfer in rib roughened tubes. Num Heat Transf Part A Appl 1989;15:165–79.
[69] Gee DL, Webb RL. Forced convection heat transfer in helically rib-roughened tubes. Int J Heat Mass Transf 1980;23:1124–36.
[70] Thianpong C, Yongsiri K, Nanan K, Eiamsa-ard S. Thermal performance evaluation of heat exchangers fitted with twisted-ring turbulators. Int Commun Heat Mass Transf 2012;39:861–8.
[71] Eiamsa-ard S, Wongcharee K, Eiamsa-ard P, Thianpong C. Heat transfer enhancement in a tube using delta-winglet twisted tape inserts. Appl Therm Eng 2010;30:310–8.
[72] Smith E, Koolnapadol N, Promvonge P. Heat transfer behavior in a square duct with tandem wire coil element insert. Chin J Chem Eng 2012;20:863–9.